

The use of COSMO-SkyMed[©] SAR data for coastal management

Guido Benassai · Maurizio Migliaccio ·
Ferdinando Nunziata

Received: 24 June 2014 / Accepted: 11 February 2015 / Published online: 20 February 2015
© JASNAOE 2015

Abstract In this paper, high spatial resolution wind fields retrieved by the synthetic aperture radar (SAR) remotely sensed images are first analyzed to force coastal wind–wave oceanographic models. A very effective technique is here proposed to retrieve wind field by SAR images collected by the Italian Cosmo-SkyMed (CSK) constellation. The technique is first calibrated using a large data set of CSK SAR data and then applied to a meaningful set of CSK SAR data collected during three storms occurred in the Southern Tyrrhenian Sea area during the winter season of 2010. CSK SAR winds are used to force SWAN wave numerical simulations to retrieve meaningful wave parameters (e.g., significant wave height, wave directions and periods) as physical descriptors of storm events. Experimental results, undertaken using both CSK and conventional ECMWF wind forcing, buoys and scatterometer winds, demonstrate that CSK winds can be successfully used to predict wave parameters during storm events. The best results are obtained when CSK winds are merged with ECMWF ones to generate a new “blended” wind product.

Keywords SWAN model · Numerical simulations · X-band COSMO-SkyMed SAR data

1 Introduction

The physical, chemical and biological interactions between the ocean and the atmosphere are of great applicative

relevance since they affect climate variability and the Earth system dynamics [1, 2]. In fact, the oceans and the atmosphere have the capability to store and exchange energy in the form of heat, moisture, and momentum, whose changes affect the climate engine of the whole planet on a large space–temporal scale. The monitoring and the forecasting of wind–wave interaction processes become particularly critical along the coastal areas, which are highly dynamic and geomorphologically complex systems that respond in a non-linear manner to extreme weather conditions and, more generally, to external perturbations [3]. Moreover, the impact of climate change along the coastal regions may include the presence of events that severely affect the Earth system dynamics, such as the possible increase of sea surface temperatures as well as the changes in frequency, intensity and duration of wave storms [4]. Based on this rationale, the evolution of winds, waves and the wind-driven sea circulation is of great applicative relevance not only for the modeling and the forecasting of both weather and climate, but even for the observation of oceanographic phenomena (e.g., floods, storms and tides activities) and coastal vulnerability assessment processes.

With respect to the wind wave modeling, advanced spectral models known as third-generation models have been developed and validated in the last decades to solve the spectral action balance equation without any a priori spectrum restrictions for the evolution of the wave growth [5–8]. These models are able to describe the physical processes of wave generation, dissipation and wave–wave interaction, overcoming the constraints of first- and second-generation wind wave models. Moreover, third-generation models predict directional spectra and wave properties, such as significant wave height, mean wave direction and frequency, swell wave height and mean direction, and wind stress fields.

G. Benassai (✉) · M. Migliaccio · F. Nunziata
Department of Engineering, University of Naples Parthenope,
Centro Direzionale Is. C4, 80143 Naples, Italy
e-mail: benassai@uniparthenope.it
URL: <http://www.ingegneria.uniparthenope.it>

All the wind wave models described above require the knowledge of sea state currents as initial information. The analysis of sea state conditions can be obtained through data assimilation, where buoy or satellite altimeter measurements are combined with a background guess from a previous forecast or climatology to create the best estimate of the current conditions. It is well known that results from wind wave simulations critically depend on the quality of the driving wind fields, whose uncertainties severely impact the estimated wave properties [9, 10]. In addition to the classical forcing provided by forecasting and/or climatological winds, other sources of wind field information have been considered in the literature to force wind wave models. Satellite-based microwave remote sensing, offering an almost all-weather and synoptic view of the observed scene both day- and night-time, is a key alternative source of information for earth observation (EO) purposes. The key instrument is the scatterometer, a non-imaging radar that provides mesoscale wind information on a daily basis. Scatterometer winds are provided as two-dimensional maps characterized by a low spatial resolution (several km). In addition, very often there is a lack of wind information near coastal area due to coast-sea spillover effects. Within this context, synthetic aperture radar (SAR), can be a valuable alternative [11–14]. The SAR is a microwave imaging radar that provides images of the observed scene that call for a spatial resolution ranging from few meters up to hundred of meters. However, since the SAR is not specifically conceived for sea surface wind field estimation, SAR wind retrieval is not at all straightforward. In addition, SAR revisit time is significantly larger than the scatterometer one.

The ability to retrieve wind fields from synthetic aperture radar images represents an important improvement for applications where knowledge of the wind field at fine spatial scales is crucial. SAR wind fields have made conspicuous marine atmospheric phenomena that were known to exist, but were previously difficult to measure and monitor. For example, the location of synoptic scale and mesoscale fronts and vortices, including hurricanes and polar and mesoscale cyclones have been identified. Moreover, additional mesoscale and microscale phenomena such as cellular convection, roll vortices, gravity waves, gap flows, barrier jets, and von Karman vortices can be observed. The synoptic remote sensing information of oceanographic and environmental parameters has raised some coastal management issues, among which the sustainability for aquaculture in areas occupied by offshore wind farms [15].

In this study, SAR measurements collected by the Italian COSMO-SkyMed (CSK) SAR constellation are exploited to provide wind information that are used to force coastal wind wave models. CSK, being a constellation of four satellites equipped with high-performance X-band SARs, provides a dense revisit time (<12 h) [16]. In addition, a tailored inversion technique is here proposed to estimate

wind field by CSK SAR images. Finally wind fields are used to force the wave model to predict key parameters. Experiments consist of numerical simulations undertaken running the SWAN model considering some relevant wave storms. The test area is the Southern Tyrrhenian coastal area and storms were recorded during the winter season in 2010. Wind information obtained by both CSK SAR and conventional scatterometer, ECMWF and buoy sources is used to force the SWAN model that provides the physical descriptors of the storm events (e.g., significant wave height, wave directions and periods). Hence, experimental results forcing the SWAN model using CSK winds are contrasted with those obtained using conventional buoys and ECMWF winds.

The main outcomes can be summarized as follows:

1. Wind information can be successfully inferred by CSK SAR data. In this study, wind speed and direction estimations are addressed separately. This implies that, unlike conventional geophysical model function (GMF) techniques, in this case no priori wind direction information is needed to estimate wind speed.
2. Wind information retrieved by CSK SAR data, when combined to ECMWF data to construct a “blended product”, provides best estimates of storm’s parameters.
3. With respect to the surface wave modeling, a multiple-connected modeling system specifically conceived for wave forecast was used in the considered coastal area, based on the Wave Watch III (WW III) model, the well-known third-generation wave model developed at NOAA/NCEP [4, 17, 18] which is operational since January 2005 at the University Parthenope [4]. Outputs from the model include significant wave height on gridded fields, with the associated wave directions and periods, and spectral information about wave energy at different wavelengths. The model was coupled with PSU/NCAR mesoscale model (MM5/WRS), which gives wind forcing at 1-h intervals, and was implemented using a nested grid configuration covering the Mediterranean Sea until the Southern Thyrrenian Sea, to produce numerical simulations of relevant wave storms. Since a coastal application was needed, the SWAN model was run, which is based on the WW III taking also into account the shoaling and refraction terms in the coastal zone [18].

2 Methods

2.1 Wind field retrieval

The SAR-based wind field retrieval is accomplished by means of a two-step procedure, which allows estimating the sea surface wind speed and wind direction,

independently. A preliminary pre-processing is undertaken on the CSK SAR data that includes land masking [19].

The SAR-based wind speed estimation is accomplished by means of a SAR wind speed algorithm based on the Azimuth cut-off procedure [20–22] which allows consistently retrieving the sea surface wind speed without requiring both any a priori wind direction information and the calibration accuracy of SAR normalized radar cross section (NRCS) measurements of the observed scene. The physical rationale at the basis of the proposed approach lies on the well-known azimuthal Doppler mis-registration due to the orbital motion of sea surface waves, which affects the sea surface SAR imaging, based on both sensor's parameters (e.g., platform altitude, velocity, etc.) and sea state conditions [20–22]. It limits the shortest detectable wavelength in the azimuth direction λ_c , which has been demonstrated to be a key kinematic parameter that, accounting for sea waves orbital motions within SAR integration time can be considered a robust indicator of the sea surface wind speed [20–22]. Based on this rationale, a SAR wind speed algorithm based on the Azimuth cut-off procedure has been developed and tested for C-band SAR measurements only where λ_c is retrieved from the noise-free SAR auto-correlation function (ACF) and physically related to the sea surface wind speed according to the following linear semi-empirical model:

$$U_{10} = \alpha (\lambda_c - A) \quad (1)$$

where U_{10} (m/s) is the wind speed at 10 m above the sea surface, A (m) is the SAR nominal azimuth resolution and α (1/s) is an empirical parameter.

Following this theoretical background, the physical rationale at the basis of the Azimuth cut-off procedure has been successfully extended and tested to the X-band VV-polarized Level 1B DGM ScanSAR Huge Region mode CSK SAR measurements [19, 23]. Hence, Eq. 1 is specified for CSK SAR data. On this purpose, a CSK SAR data set consisting of 60 X-band VV-polarized Level 1B Detected Ground Multi-look (DGM) ScanSAR Huge Region mode CSK SAR measurements collected in the Southern Tyrrhenian Coastal area on 2010 is used to calibrate Eq. 1, i.e., to find α and λ_c [19–23]. The ground truth, which is used as reference wind field for both comparison and validation purposes, is provided by timely and spatially co-located ASCAT scatterometer wind fields (freely available at <http://podaac.jpl.nasa.gov>), with a spatial gridding resolution of 12.5×12.5 km. In the particular case where the ASCAT scatterometer ground truth is not available for the CSK SAR acquisition, the reference ground truth is then provided by European Centre for Medium Weather Forecast (ECMWF) model data (available at: <http://www.ecmwf.int/>), with a spatial resolution of 0.2°

(20×20 km). Since the reference ground truth wind field (both the ASCAT scatterometer and the ECMWF model ones) is not always both timely co-located with respect to the SAR image acquisition, a linear interpolation in time is accomplished between the ground truth reference wind field data acquired before and after the SAR acquisition time, thus providing the timely co-located reference wind field. Moreover, since the reference ground truth is available at the given resolution gridding scale of both 12.5×12.5 and 20×20 km for the ASCAT scatterometer and the ECMWF model wind field, respectively, a bi-linear spatially interpolation of the timely co-located wind field is accomplished inside of the spatial domain of SAR image at the specific SAR sub-image gridding scale ($N \times N$) used for wind field retrieval purposes. Some results are summarized in the scatter plots of Fig. 1, where the 12.5×12.5 km SAR-based wind speed and 6.25×6.25 km wind speed retrievals are consistently compared with respect to the corresponding ASCAT scatterometer reference wind speed, respectively, for the whole processed CSK SAR data set. Calibration results are summarized in Fig. 1a where CSK wind speed is contrasted with ASCAT scatterometer reference ground truth. In detail, the inter-comparison results in a mean error (μ) value of -0.73 m/s, a standard deviation (σ) value of 2.07 m/s and an RMSE value of 2.19 m/s.

The SAR-based wind direction estimation is accomplished by means of a SAR wind direction retrieval procedure based on the multi-resolution analysis of the discrete wavelet transform (WT-MRA) [24, 25]. The physical rationale of this technique accounts for sea–air interaction processes and is focused on the theory that sea surface wind direction retrieval lies on the measurements of texture features in SAR images over the sea. The proposed approach aims at retrieving the orientations of atmospheric boundary layer (ABL) rolls, which are often present in SAR images and appear as sea surface streaks at kilometer scales.

Figure 1b contrasts the wind directions estimated by CSK SAR with ASCAT reference ground truth. The scatterplot shows a mean error (μ) value of 1.71° , a standard deviation (σ) value of 18.88° and an RMSE value of 18.95° .

These results effectively demonstrate the consistency of X-band CSK SAR-derived wind field retrievals with respect to the ASCAT scatterometer ground truth. Such results demonstrate the effectiveness of both the X-band Azimuth cut-off model function and the WT-MRA technique presented in pre-processing analysis to get consistent wind speed and wind direction estimation, respectively. Furthermore, experimental results show the full benefits of X-band Level 1B DGM ScanSAR Huge Region mode CSK SAR data as alternative source of wind field estimation.

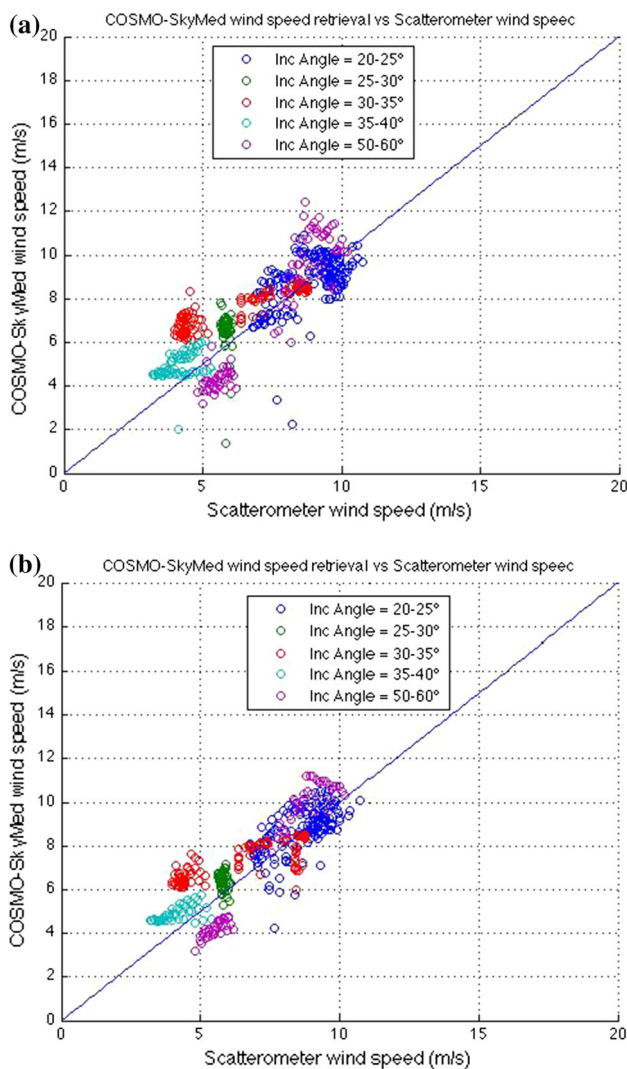


Fig. 1 Probability density scatter plot comparison between the X-band CSK SAR-derived wind field estimation and the ASCAT scatterometer reference ground truth, for the whole processed CSK SAR data set. **a** 12.5 × 12.5 km, **b** 6.25 × 6.25 km. The inter-comparison shows a mean error, a standard deviation and a rmse equal to −0.73, 2.07 and 2.19 m/s, respectively, when dealing with wind speed (**a**). When dealing with wind direction, the mean error, the standard deviation and the rmse are equal to 1.71°, 18.88° and 18.95°, respectively

2.2 SWAN model

The SWAN model is a third-generation numerical wave model, which allows computing random, short-crested waves in coastal regions with shallow water and ambient currents [7, 8] which describes the temporal and spatial variation of the wind-induced surface elevation, the white-capping effects and the friction with the sea bottom layer. In SWAN the waves are described with the two-dimensional wave action density spectrum $N = F/\sigma$, even when non-linear phenomena dominate (e.g., in the surf zone).

The action density spectrum N is considered rather than the energy density spectrum $E(\sigma, \theta)$, since in the presence of ambient currents only the action density is conserved [9]. The evolution of the wave spectrum is described by the spectral action balance equation [7].

The model is typically forced by using the wind field forcing at 1-h intervals provided through the advanced research weather research and forecast (WRF-ARW) wind field model data, i.e. the next-generation mesoscale numerical weather model predictions that are designed to serve both operational forecasting and atmospheric research needs. The model is implemented on nested grids, with an implicit numerical propagation scheme, which implies that the computations are more economic in shallow water [7–10]. Outputs from the SWAN model include significant wave height (H_s) on gridded fields, with the associated wave directions (D_w) and periods (T_p), and the wave energy spectral information at different wavelengths. The generation and propagation equation is given by:

$$\frac{\partial}{\partial t} N + \frac{\partial}{\partial x} c_x N + \frac{\partial}{\partial y} c_y N + \frac{\partial}{\partial \sigma} c_\sigma N + \frac{\partial}{\partial \theta} c_\theta N = \frac{S}{\sigma} \quad (2)$$

where S is the effect of the difference between the inner and the outer energy for the spectrum F and σ is the intrinsic frequency. The first term on the left-hand side of Eq. 2 represents the timely-change rate of the local action density spectrum. The second and third term on the left-hand side of Eq. 2 represents the propagation of the action density spectrum in the Cartesian coordinates space, with propagation velocities c_x and c_y . The fourth term on the left-hand side of Eq. 2 represents the shifting of the relative frequency in the action density spectrum due to variations in depths and currents, with a propagation velocity c_σ . The fifth term on the left-hand side of Eq. 2 represents both the depth- and the current-induced refraction of the local action density spectrum, with propagation velocity c_θ . The term at the right-hand side of the action balance Eq. 2 is the source term of the energy density, representing the effects of generation, dissipation, and non-linear wave–wave interactions.

The SWAN model has been operational at University Parthenope since January 2005 and has been adopted for simulating both waves’ generation and propagation in the Gulf of Naples. The model is typically forced using the wind field at 1-h intervals provided by the WRF-ARW wind field model data, i.e., the next-generation mesoscale numerical weather model predictions that are designed to serve both operational forecasting and atmospheric research needs [4, 7, 8, 18]. The model is implemented on nested grids, with a numerical propagation scheme, which makes the numerical code quite effective in shallow water [4, 7, 8, 18]. Outputs of the SWAN model include significant wave height (H_s) on gridded fields, with the

associated wave directions (D_{SW}) and periods (T_p), and the wave energy spectral information at different wavelengths.

3 Experimental results

Experiments are undertaken running SWAN model with respect to three relevant storms recorded in the test area during the winter season of 2010. The test area is the coastal zone of the southern Tyrrhenian Sea, including the Gulfs of Gaeta, Napoli, Salerno and Policastro, which are of great applicative relevance for both oceanographic and coastal-maritime surveillance purposes, see Fig. 2 where an example of SAR data collected in this area is shown. Wind forcing is provided by both CSK SAR data and conventional sources: ECMWF, buoys and scatterometer. Moreover, a blended product that consists of ECMWF winds merged with CSK ones is used.

3.1 Wind retrieval

Wind retrieval consists of applying the two-step scheme to three CSK SAR data relevant to the storms under investigation. Three cases are investigated: the storms of 9, 10 November 2010, 17, 18 December 2010 and 23–25 December 2010. Wind speed is retrieved from CSK SAR data collected during the storms using the calibrated Eq. 1. Wind direction is estimated using WT-MRA approach.

3.2 Wave simulations

In this sub-section, sea wave numerical simulations of SWAN model are described with respect to some relevant wave storms recorded in the considered test area during the winter season of 2010. Table 1 gives the main characteristics of the wave storms; Table 2 gives the mean and standard deviations of the simulated and recorded H_s during the storms.

An example of the SWAN output is given in Fig. 3 with reference to the #3 storm of December 2010, in which the SAR data spatial domain reported in Fig. 2 is evidenced.

A first meaningful set of results relevant to the application of SWAN model is shown in Fig. 4 where the wave storm of 8–10 November 2010 is addressed.

In this case, neither the maximum wave heights nor the time evolution of the storm are properly simulated with the wind field forcing provided by ECMWF model winds. In fact, the maximum values of H_s , which are obtained by using both ECMWF model winds and buoys wave field data only, are 5.5 and 4.0 m, respectively, which are shifted 15 h earlier. The use of a blended wind field product provided by CSK SAR-derived wind field estimations and ECMWF model winds gives more accurate results, with an

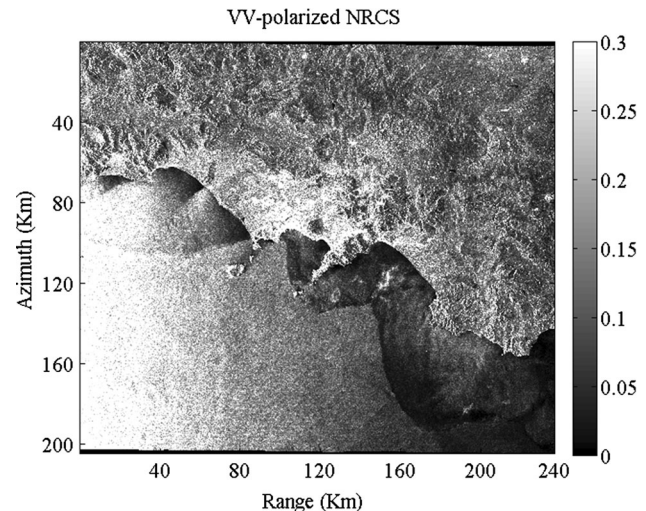


Fig. 2 An example of VV-polarized Level 1B Multi-Look Ground Detected (DGM) ScanSAR Huge Region CSK© SAR data, gathered in the test area

Table 1 Wave storms of the winter season 2010, used for sea wave numerical simulations

Storm	Date	H_s (m)	T_p (s)	D_w ($^\circ$ N)
#1	Nov 8–10th 2010	4.23	9.5	218
#2	Dec 17–18th 2010	5.01	9.5	231
#3	Dec 23–25th 2010	4.29	10.0	255

Significant wave height, peak period and wave direction at the storm peak are reported

underestimation of 0.5 m in H_s (3.5 m out of 4.0 m), a more accurate resemblance of the storm and a lower temporal shift, as confirmed by inspection of Fig. 4 and Table 2. In fact Table 2 shows that the mean value of the simulated H_s with the blended winds (2.76 m) is close to the ground truth one (2.89 m).

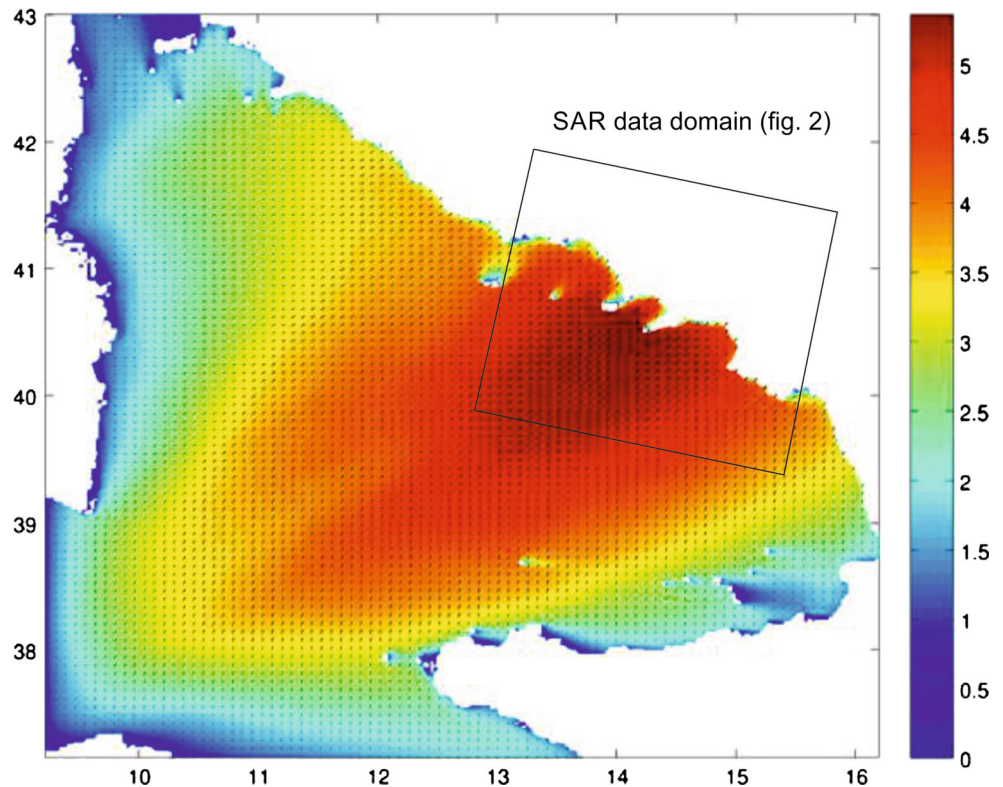
A second meaningful set of results relevant to the application of SWAN model is shown in Fig. 5 where the wave storm of 17, 18 December 2010 is addressed (see Table 1). The sea wave numerical simulation accomplished by using the blended CSK–ECMWF wind field products shows that the CSK SAR-derived wind field estimations are able to catch the changing storm characteristics, although the peaks of the wave storm are quite underestimated. In fact, the blended wind field product provided by CSK SAR-derived wind field estimations and ECMWF model winds retrieves the peak value of H_s , which numbers 3.5 m, instead of 5.0 m.

This result is less accurate than the one obtained by using a wind field forcing provided by ECMWF model winds only, mainly because of the lower time resolution of the wind data and in spite of the higher spatial resolution. In fact, the wave storm event presents a quite fast time

Table 2 Mean and standard deviation of simulated and recorded H_s during the wave storms of the winter season 2010

Storm	Date	Wave buoy		ECMWF winds		SAR winds		Blended winds	
		Mean	SD	Mean	SD	Mean	SD	Mean	SD
#1	Nov 8–10th 2010	2.89	0.54	3.60	1.06	2.07	0.12	2.76	0.50
#2	Dec 17–18th 2010	2.60	1.41	2.56	0.66	1.42	0.82	1.43	0.99
#3	Dec 23–25th 2010	2.97	0.64	3.10	0.80	1.70	0.56	2.20	0.76

Fig. 3 Simulation of #3 storm of December 2010 on the numerical domain



evolution, which cannot be interpreted by using wind field data with a temporal interval of 12–24 h. Table 2 shows that the mean value of the simulated H_s with the ECMWF winds (2.56 m) resembles the ground truth one (2.60 m).

Compared to both buoys wave field observations and ECMWF model winds, very effective results are obtained with the blended wind field products provided by CSK SAR-derived wind field estimations and ECMWF model winds. More generally, numerical simulations demonstrate that the SWAN model allows providing significant and accurate sea wave estimations even by using blended wind field product composed by both model and remotely sensed wind field data.

A third meaningful set of results relevant to the application of the SWAN model is shown in Fig. 6, where the wave storm of 23–25 December 2010 (see Table 1) is

addressed. Numerical simulations agree with previous experimental results. In particular, the blended wind field product provided by CSK SAR-derived wind field estimations and ECMWF model winds allows improving the retrieval of the SWAN-based wind–wave interaction parameters especially in the first part of the wave storm, where numerical simulations accomplished with ECMWF model winds tends to provide an H_s value overestimation. Moreover, when a blended product is considered, better results are obtained with a little underestimation (25 %) of the mean H_s (see Table 2).

Hence, with regard to the storm reconstruction, experimental results demonstrate that sea wave numerical simulations accomplished with blended CSK-ECMWF wind field forcing closely follow the true significant wave height of the wave storms.

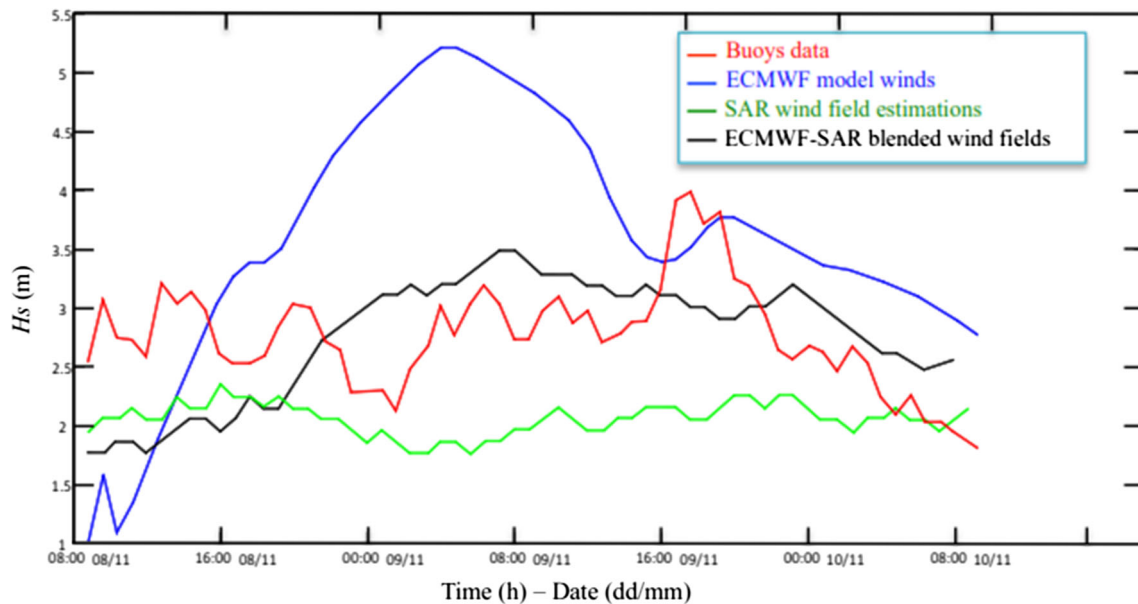


Fig. 4 Simulated and measured H_s for the winter storm of 9–10 November 2010. Comparison among buoys (blue), blended buoys and ECMWF (red), COSMO-SkyMed© SAR (green), and blended buoys and COSMO-SkyMed© SAR-derived wind fields (black) (color figure online)

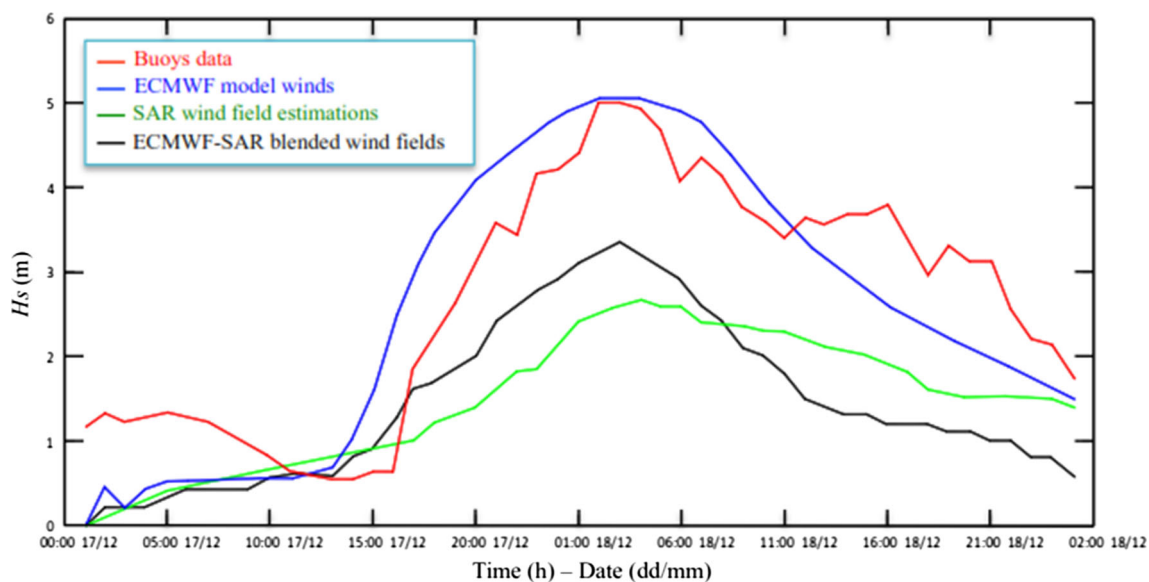


Fig. 5 Simulated and measured H_s for the winter storm of 17–18 December 2010. Comparison among buoys (red), blended buoys and ECMWF (blue), COSMO-SkyMed© SAR (green), and blended buoys and COSMO-SkyMed© SAR-derived wind fields (black) (color figure online)

This important result can be used for further research relevant to the use of CSK SAR data as alternative integrated source of sea surface wind field information. Furthermore, experimental results effectively demonstrate that a blended wind product including both ECMWF model data and CSK SAR-derived wind field estimations can provide valuable improvements of wind–wave interaction modeling.

4 Discussion

The results of numerical simulations can be summarized as follows:

- Numerical simulations carried out with ECMWF model winds properly describe the sea storms at the peak with respect to the significant wave heights H_s .

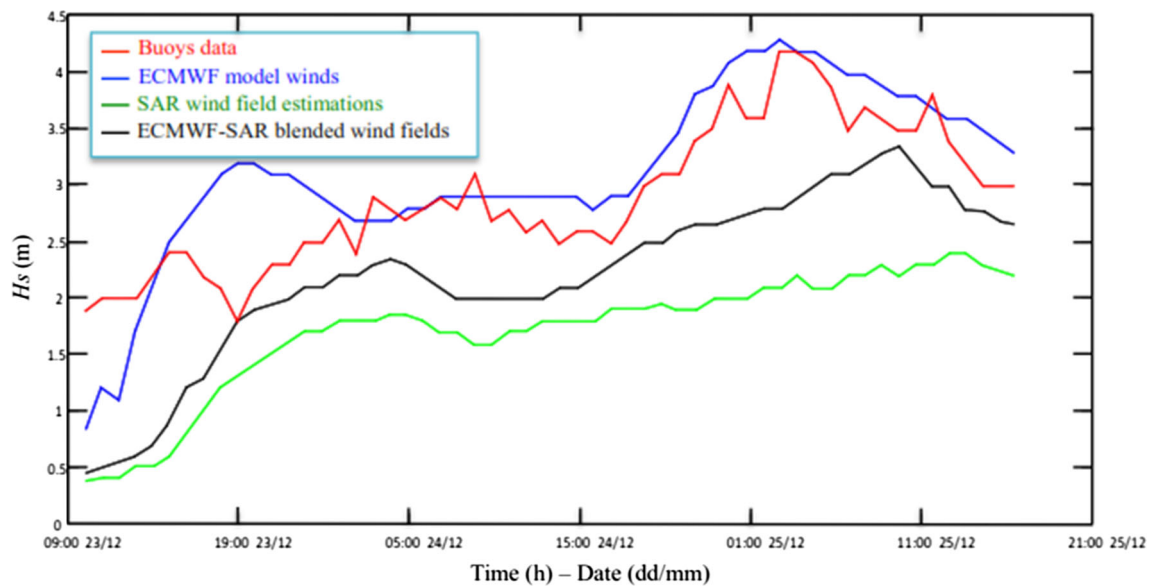


Fig. 6 Simulated and measured H_s for the winter storm of 23–25 December 2010. Comparison among buoys (red), blended buoys and ECMWF (blue), blended COSMO-SkyMed© SAR and ECMWF

(black), and blended buoys and COSMO-SkyMed© SAR-derived wind fields (green) (color figure online)

The only exception is represented by the first wave storm (see Fig. 4; Table 2), where the peak value of H_s is 38 % overestimated and the mean value of H_s is 25 % overestimated. With respect to the wave storm duration, the first two storms are properly described (see Figs. 4 and 5, respectively; Table 1), while the third one exhibits an overestimation of 9 % (see Fig. 6; Table 1).

- b. Numerical simulations carried out with a blended wind field product provided by ECMWF model winds and COSMO-SkyMed© SAR-derived wind field estimations better follow the significant wave heights at the peak for the first wave storm (Fig. 4; Table 1), while for the other two wave storms there is an underestimation of the peak H_s of 32 and 15 %, respectively, (Figs. 5, 6) and of the mean H_s of 45 and 25 %, respectively (Table 2). Taking into account the wave storm duration, the results agree with the buoys wave field data for both the first and third wave storms (Figs. 4, 6, respectively; Table 1) and give an underestimation of 37 % for second wave storm (Fig. 5; Table 1).

5 Conclusions

In this paper, X-band CSK SAR data are successfully experimented as wind field forcing of wave oceanographic modeling for sea wave numerical simulation in a coastal environment. The wind–wave oceanographic modeling is

based on the third-generation SWAN model, run with the different data.

With respect to the storm reconstruction, experimental results demonstrate that the sea wave numerical simulations accomplished with blended CSK-ECMWF wind field forcing closely follow the true significant wave height of the first wave storm (see Tables 1, 2). In fact, with regard to the mean values, a slight H_s underestimation of 4 % is provided against the 25 % of the wave simulations accomplished with ECMWF model wind forcing only. However, for the other two wave storms (i.e., the second and the third ones in Table 1), experimental results provide a peak H_s underestimation of 32 and 15 %, respectively, which is even higher in the mean values.

Experimental results first show how X-band CSK SAR-derived wind field estimations can be effectively used to force the SWAN coastal wave model for oceanographic applications. Meaningful tests are successfully accomplished in the Southern Tyrrhenian Sea basin, where some significant wave storms have been both recorded and analyzed. This is of both scientific and operational relevance.

Acknowledgments COSMO-SkyMed© SAR data used in this study are provided by Italian Space Agency under the scientific research project entitled “Improvement of Oceanic Modelling for Coastal Management by means of COSMO-SkyMed© SAR data” (Project ID 1500). The project, funded by Italian Space Agency (ASI) aims at using SAR-derived wind fields to force surface wave models in a coastal environment, and to validate them with wind data sets provided by scatterometer and wave data set provided by in situ wave buoys. The research group is formed by a telecommunication engineering team for retrieving SAR image formation and wind

scatterometer data inversion, and a coastal engineering team for the wave and coastal hydraulics modeling, the data validation and the following management applications (coastal risk assessment).

References

- Janssen P (2004) *The interaction of ocean waves and wind*. Cambridge University Press, UK
- Harlan Jr JA (2005) Short time scale effects on high frequency radar-derived current velocity measurements. PhD Dissertation, University of Colorado at Boulder
- Di Paola G (2011) Geological and geo-morphological characterization of coastal Sele Plain (Campania, Italy) and considerations about its vulnerability. PhD Thesis, Università degli Studi del Molise, Italy
- Benassai G (2006) Introduction to coastal dynamics and shoreline protection, vol 1. Wit Press, Southampton, pp 1–356
- WAMDI Group (1988) The WAM model—a third generation ocean wave prediction model. *J Phys Oceanogr* 18:1775–1810
- Tolman HL (1991) A third-generation model for wind waves on slowly varying, unsteady and inhomogeneous depths and currents. *J Phys Oceanogr* 21:782–797
- Booij N, Ris RC, Holthuijsen LH (1999) A third-generation wave model for coastal regions, part I: model description and validation. *J Geophys Res* 104:7649–7666
- Benassai G, Ascione I (2006) Implementation and validation of Wave Watch III model offshore the coastlines of Southern Italy. In: *Proceedings of 25th OMAE 2006*, Hamburg, Germany, 4–9 June 2006, pp 553–560
- Teixeira J, Abreu M, Soares C (1995) Uncertainty of ocean wave hindcasts due to wind modelling. *J Offshore Mech Arct Eng* 117:294–297
- Holthuijsen L, Booij N, Bertotti L (1996) The propagation of wind errors through ocean wave hindcasts. *J Offshore Mech Arct Eng* 118:184–189
- Johannessen OM, Sandven S, Jenkins AD, Durand D, Pettersson LH, Espedal H, Evensen G, Hamre T (2000) Satellite earth observation in operational oceanography. *Coast Eng* 41:155–176
- Portabella M (2002) Wind field retrieval from satellite radar systems. PhD Thesis, University of Barcelona, ISBN: 90-6464-499-3
- Monaldo FM, Thompson DR, Winstead NS, Pichel WG, Clemente-Colon P, Christiansen MB (2005) Ocean wind field mapping from synthetic aperture radar and its application to research and applied problems, Johns Hopkins. *Appl Tech Dig* 26:102–113
- Yang X, Li X, Pichel WG, Li Z (2011) Comparison of ocean surface winds from ENVISAT ASAR, MetOp ASCAT Scatterometer, Buoy measurements, and NOGAPS model. *IEEE Geosci Remote* 49:4743–4750
- Benassai G, Mariani P, Stenberg C, Christoffersen M (2014) A sustainability index of potential co-location of offshore wind farms and open water aquaculture. *Ocean Coast Manag* 95:213–218. ISSN: 0964-5691. doi:10.1016/j.oceacoaman.2014.04.007
- Italian Space Agency (ASI)—COSMO-SkyMed Mission, 2007. COSMO-SkyMed system description and user guide [Online]. Available: <http://www.asi.it/it/flash/osservare/cosmoskymed>
- Tolman HL (2009) User manual and system documentation of WAVEWATCH III version 3.14, NOAA/NWS/NCEP/MMAB Technical Note 276, 194
- Holthuijsen LH, Booij N, Ris RC (1993) A spectral wave model for the coastal zone. In: *Proceedings of the 2nd international symposium on ocean wave measurement and analysis*, New Orleans, pp 630–641
- Migliaccio M, Montuori A, Nunziata F (2012) X-band Azimuth cut-off for wind speed retrieval by means of COSMO-SkyMed SAR data. In: *Proceedings of IEEE/OES Baltic international symposium*, Klaipėda, Lithuania
- Chapron B, Fouhaily TE, Kerbaol V (1995) Calibration and validation of ERS wave mode products, Inst Fr De Rech pour l'Exploit. de la Mer, Brest, France, Doc. DRO/OS/95-02
- Kerbaol V, Chapron B, Vachon PW (1998) Analysis of ERS-1/2 synthetic aperture radar wave mode images. *J Geophys Res* 103:7833–7846
- Korsbakken E, Johannessen JA, Johannessen OM (1998) Coastal wind field retrievals from ERS synthetic aperture radar image. *J Geophys Res* 103:7857–7874
- Montuori A, Migliaccio M, Nunziata F (2012) Wind speed estimation in the tyrrhenian sea by means of X-band COSMO-Sky-Med SAR Data. In: *Proceedings of tyrrhenian workshop on advances in radar and remote sensing*, Naples, Italy
- Du Y, Vachon PW, Wolfe J (2002) Wind direction estimation from SAR images of the ocean using wavelet analysis. *Can J Remote Sens* 28:498–509
- Schiavulli D, Sorrentino A, Migliaccio M (2012) An Innovative Technique for Postprocessing Descalloping. *IEEE Geosci Remote S* 99:1–4